H_2S: A Universal Defense Against Antibiotics in Bacteria

Konstantin Shatalin, *et al.*

Science **334**, 986 (2011);
DOI: 10.1126/science.1209855

the possibility that the control of oxidant stress may be a common mechanism.

To investigate the effect of targeting the SR to increase antibiotic activity in lethal infections, we infected mice with stationary-phase *P. aeruginosa*. Whereas ofloxacin failed to increase the survival of mice infected with wild-type bacteria, it was highly effective against the Δ*relA spoT* strain (Fig. 4A). Furthermore, eliminating HAQ biosynthesis abolished the susceptibility of the mutant in vivo (Fig. 4A), as was seen in vitro (Fig. 2E). Inactivation of the SR also increased antibiotic activity in a murine bioflm model (Fig. 4B). Finally, because tolerance allows bacteria to survive sustained drug exposure, tolerant subpopulations are thought to be an important source of genetic antibiotic-resistant mutants (*9*, *24*). As shown in Fig. 4C, SR inactivation eliminated the emergence of ofloxacin-resistant clones in conditions promoting adaptive resistance.

Whether cells recognize it or not, starvation will eventually stop growth and the activity of antibiotic targets. However, the capacity to sense and respond to starvation allows bacteria to arrest growth in a regulated manner that maximizes chances for long-term survival. Our data show that interfering with this orderly process sensitizes experimentally starved, stationary-phase, and biofilm bacteria to antibiotics, without stimulating their growth. Furthermore, our experiments suggest that starvation responses protect by curtailing the production of prooxidant metabolites and increasing antioxidant defenses. Thus, antibiotic-tolerant states may depend on physiological adaptations without direct connections to antibiotic target activity or to drug uptake, efflux, or inactivation. Identifying these adaptations, and targeting them to enhance the activity of existing drugs, is a promising approach to mitigate the public health crisis caused by the scarcity of new antibiotics.

References and Notes

1. R. H. Eng, F. T. Padberg, S. M. Smith, E. N. Tan, C. E. Cherubin, *Antimicrob. Agents Chemother.* **35**, 1824 (1991).
2. J. C. Batten, P. A. Dineen, R. M. McCune Jr., *Ann. N. Y. Acad. Sci.* **65**, 91 (1956).
3. W. McDermott, *Yale J. Biol. Med.* **30**, 257 (1958).
4. M. R. Parsek, P. K. Singh, *Annu. Rev. Microbiol.* **57**, 677 (2003).
5. C. A. Fux, J. W. Costerton, P. S. Stewart, P. Stoodley, *Trends Microbiol.* **13**, 34 (2005).
6. K. Lewis, *Nat. Rev. Microbiol.* **5**, 48 (2007).
7. P. S. Stewart, M. J. Franklin, *Nat. Rev. Microbiol.* **6**, 199 (2008).
8. G. Borriello, L. Richards, G. D. Ehrlich, P. S. Stewart, *Antimicrob. Agents Chemother.* **50**, 382 (2006).
9. B. R. Levin, D. E. Rozen, *Nat. Rev. Microbiol.* **4**, 556 (2006).
10. M. Cashel, D. R. Gentry, V. J. Hernandez, D. Vinella, in Escherichia coli *and* Salmonella, F. C. Neidhardt, Ed. (ASM Press, Washington, D.C., 1996), vol. 1, pp. 1458-1496.
11. M. F. Traxler *et al.*, *Mol. Microbiol.* **68**, 1128 (2008).
12. S. L. Vogt *et al.*, *Infect. Immun.* **79**, 4094 (2011).
13. Materials and methods are available as supporting material on *Science* Online.
14. M. A. Kohanski, D. J. Dwyer, B. Hayete, C. A. Lawrence, J. J. Collins, *Cell* **130**, 797 (2007).
15. D. J. Dwyer, M. A. Kohanski, J. J. Collins, *Curr. Opin. Microbiol.* **12**, 482 (2009).
16. X. Wang, X. Zhao, *Antimicrob. Agents Chemother.* **53**, 1395 (2009).
17. D. A. D'Argenio, M. W. Calfee, P. B. Rainey, E. C. Pesci, *J. Bacteriol.* **184**, 6481 (2002).
18. E. Déziel *et al.*, *Proc. Natl. Acad. Sci. U.S.A.* **101**, 1339 (2004).
19. F. Bredenbruch, R. Geffers, M. Nimtz, J. Buer, S. Häussler, *Environ. Microbiol.* **8**, 1318 (2006).
20. S. P. Diggle *et al.*, *Chem. Biol.* **14**, 87 (2007).
21. S. Häussler, T. Becker, *PLoS Pathog.* **4**, e1000166 (2008).
22. Y. Wang, D. K. Newman, *Environ. Sci. Technol.* **42**, 2380 (2008).
23. L. A. Gallagher, S. L. McKnight, M. S. Kuznetsova, E. C. Pesci, C. Manoil, *J. Bacteriol.* **184**, 6472 (2002).
24. D. F. Warner, V. Mizrahi, *Clin. Microbiol. Rev.* **19**, 558 (2006).

Acknowledgments: We thank M. Cashel, C. Manoil, and J. Burns for providing strains; A. Hunziker and J. Harrisson for technical assistance; and J. Penterman, J. Mougous, M. Parsek, and C. Manoil for helpful discussions. Funding was provided by the Burroughs Wellcome Fund (D.N. and P.K.S), Cystic Fibrosis Foundation (P.K.S), NIH (P.K.S), and Canadian Institutes for Health Research (D.N.).

Supporting Online Material

www.sciencemag.org/cgi/content/full/334/6058/982/DC1
Materials and Methods
Figs. S1 to S14
Table S1
References (*25*–*46*)

12 July 2011; accepted 27 September 2011
10.1126/science.1211037

H_2S: A Universal Defense Against Antibiotics in Bacteria

Konstantin Shatalin,[1] Elena Shatalina,[1] Alexander Mironov,[2] Evgeny Nudler[1]*

Many prokaryotic species generate hydrogen sulfide (H_2S) in their natural environments. However, the biochemistry and physiological role of this gas in nonsulfur bacteria remain largely unknown. Here we demonstrate that inactivation of putative cystathionine β-synthase, cystathionine γ-lyase, or 3-mercaptopyruvate sulfurtransferase in *Bacillus anthracis*, *Pseudomonas aeruginosa*, *Staphylococcus aureus*, and *Escherichia coli* suppresses H_2S production, rendering these pathogens highly sensitive to a multitude of antibiotics. Exogenous H_2S suppresses this effect. Moreover, in bacteria that normally produce H_2S and nitric oxide, these two gases act synergistically to sustain growth. The mechanism of gas-mediated antibiotic resistance relies on mitigation of oxidative stress imposed by antibiotics.

Until recently H_2S has been known merely as a toxic gas. It is now associated with beneficial functions in mammals from vasorelaxation, cardioprotection, and neurotransmission to anti-inflammatory action in the gastrointestinal tract (*1*–*3*). The ability of H_2S to function as a signaling molecule parallels the action of another established gasotransmitter, nitric oxide (NO) (*3*–*5*). Like NO, H_2S is produced enzymatically in various tissues (*1*–*3*). Three H_2S-generating enzymes have been characterized in mammals: cystathionine β-synthase (CBS), cystathionine γ-lyase (CSE), and 3-mercaptopyruvate sulfurtransferase (3MST). CBS and CSE produce H_2S predominantly from L-cyst(e)ine (Cys). 3MST does so via the intermediate synthesis of 3-mercaptopyruvate produced by cysteine aminotranferase (CAT), which is inhibited by aspartate (Asp) competition for Cys on CAT (*1*) (fig. S1).

In contrast to mammal-derived H_2S, bacteria-derived H_2S has been known for centuries but was considered to be only a byproduct of sulfur metabolism, with no particular physiological function in nonsulfur microorganisms. Likewise, little is known about the metabolic pathways involving H_2S in mesophilic bacteria. However, analysis of bacterial genomes has revealed that most, if not all, have orthologs of mammalian CBS, CSE, or 3MST (figs. S1 and S2), which suggested an important cellular function(s) that preserved these genes throughout bacterial evolution. We became interested in the role of these enzymes after establishing that endogenous NO protects certain Gram-positive bacteria against antibiotics and oxidative stress (*6*–*8*). Considering some functional similarities between mammalian gasotransmitters (*1*–*3*), we hypothesized that bacterial H_2S may, similarly, be cytoprotective.

To determine whether CBS, CSE, or 3MST produces H_2S in bacteria, we inactivated each enzyme genetically or chemically in four clinically relevant and evolutionarily distant pathogenic species: *Bacillus anthracis* (Sterne), *Pseudomonas aeruginosa* (PA14), *Staphylococcus aureus* (MSSA RN4220 and MRSA MW2), and *Escherichia coli* (MG1655). The first three species have the CBS/CSE operon, but not 3MST, whereas *E. coli* carries 3MST, but not CBS/CSE. The chromosomal organization of H_2S genes (fig. S3) and the strategy we used for their replacement prevented any polar effects. We monitored H_2S production in wild-type (wt) and mutant cells using lead acetate [$Pb(Ac)_2$], which reacts

[1]Department of Biochemistry, New York University School of Medicine, New York, NY 10016, USA. [2]State Research Institute of Genetics and Selection of Industrial Microorganisms, Moscow 117545, Russia.

*To whom correspondence should be addressed E-mail: evgeny.nudler@nyumc.org

specifically with H_2S to form a brown lead sulfide stain. The rate of change of staining on a $Pb(Ac)_2$-soaked paper strip is directly proportional to the concentration of H_2S (*9*). Deletion of CBS/CSE in *B. anthracis* and *P. aerugenosa* or 3MST in *E. coli* greatly decreased or eliminated PbS staining (Fig. 1A). Similar results were obtained when DL-propargylglycine (PAG), aminooxyacetate (AOAA), or Asp were used, respectively, as specific inhibitors of CSE, CBS, or 3MST (Fig. 1A). Addition of Cys markedly increased PbS staining for all wt, but not CSE-CBS– or 3MST-deficient bacteria (Fig. 1B). In addition, overexpression of the chromosomal 3MST gene from a strong pLtetO-1 promoter in *E. coli* resulted in increased production of H_2S (Fig. 1A). We conclude that all three enzymes produce H_2S endogenously from Cys during exponential growth of bacteria in rich media.

To elucidate the physiological role of H_2S, we first compared wt and 3MST-deficient *E. coli* in a phenotype microarray (PMA) (fig. S4 and table S1). Whereas these strains showed little or no growth defects (fig. S5), a large number of antibiotics, highly diverse in structure and function, preferentially suppressed growth of 3MST-deficient cells (Table 1 and table S1). The killing and growth curves obtained for wt and 3MST and CBS/CSE mutant *E. coli*, *P. aerugenosa*, *S. aureus*, and *B. anthracis* in the presence of several representative antibiotics confirmed the results of the screen and generalized them to both Gram-positive and -negative species (Fig. 1C and figs. S6 and S7). 3MST overexpression resulted in increased resistance to spectinomycin (fig. S6A), whereas chemical inhibition of CBS, CSE, or 3MST rendered bacteria more sensitive to different antibiotics (Fig. 1C and fig. S6B). An H_2S donor, NaHS, suppressed the antibiotic sensitivity of CBS-CSE– and 3MST-deficient cells (Fig. 1C and figs. S6C and S7). Taken together, these results establish that endogenously produced H_2S confers multidrug resistance.

H_2S-mediated cytoprotection resembles that of NO, which defends certain Gram-positive bacteria against some of the same antibiotics as does H_2S (*8*). NO-mediated protection relies, in part, on its ability to defend bacteria against oxidative stress imposed by antibiotics (*6*–*8*). To examine whether H_2S acts by a similar mechanism, we performed detailed analyses of its effect on bacterial killing by the representative antibiotics, gentamicin (Gm), ampicillin (Ap), and nalidixic acid (NA) (Fig. 2). All three have been shown to exert their bactericidal effect via oxidative stress (*8*, *10*). Indeed, pretreatment of cells with 2,2′-dipyridyl, an iron chelator that suppresses the damaging Fenton reaction (*11*), or the hydroxyl radical scavenger thiourea, substantially decreased the toxicity of Gm (Fig. 2A). Note that wt and H_2S-deficient cells became equally resistant to Gm in the presence of dipyridyl or thiourea (Fig. 2A). Moreover, the H_2S donor added together with Gm was as effective as dipyridyl or thiourea in protecting against antibiotics but failed to further protect cells that had already been pretreated with antioxidants (Fig. 2A). Thus, H_2S, like NO, acts by suppressing the oxidative component of antibiotic toxicity. Consistently, H_2S-generating enzymes provided protection against antibiotics only under aerobic conditions. Anaerobically grown CBS/CSE-deficient *B. anthracis* cells were as resistant to NA or pyocyanin as wt bacteria (Fig. 2B and fig. S8).

The above results suggested that H_2S bolsters the antioxidant capacity of bacterial cells. Indeed, H_2S-deficient *B. anthracis*, *E. coli*, *S. aureus*, and *P. aeruginosa* displayed higher susceptibility to peroxide than their wt counterparts, whereas NaHS rendered them more resistant to the peroxide (Fig. 2C and figs. S9 to S11).

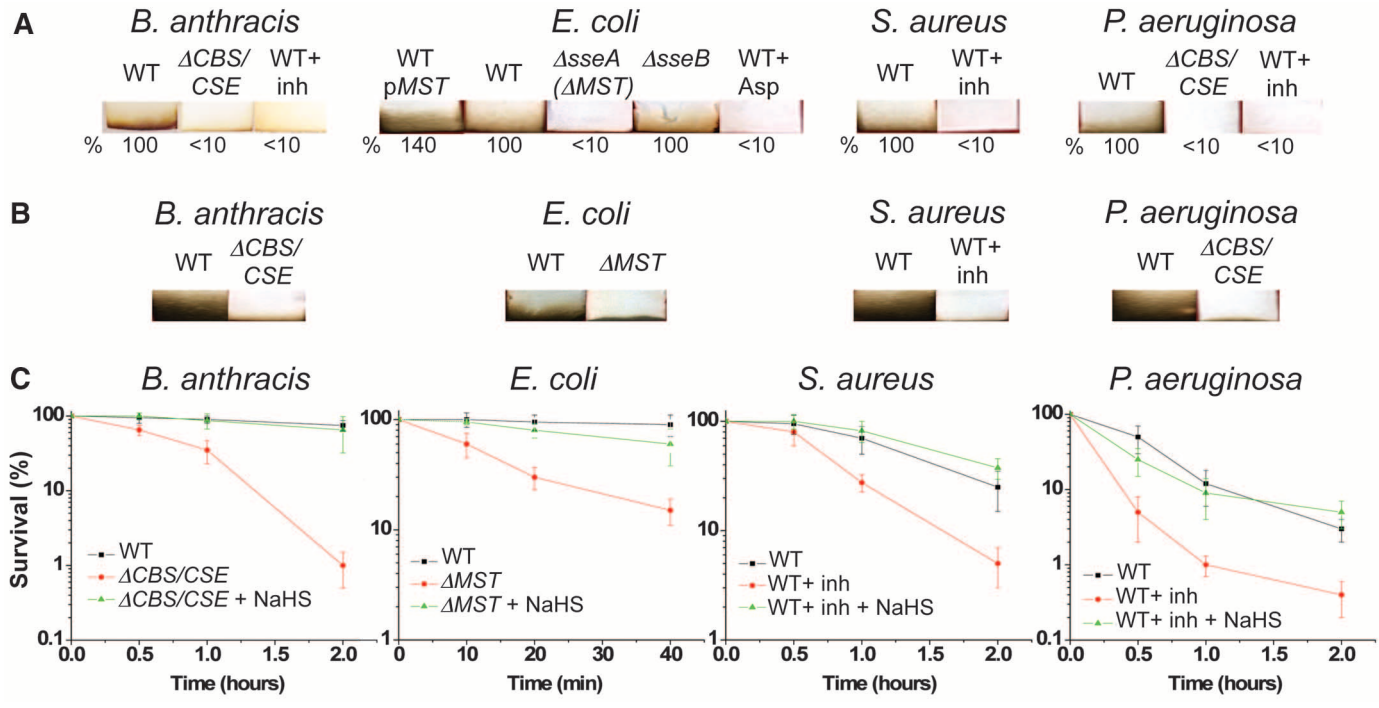

Fig. 1. Endogenous H_2S protects bacteria against antibiotic toxicity. (**A**) H_2S production by *B. anthracis*, *S. aureus*, *P. aeruginosa*, and *E. coli* depends on CBS/CSE and 3MST, respectively. Lead acetate–soaked paper strips show a PbS brown or black stain as a result of reaction with H_2S. Strips were affixed to the inner wall of a culture tube, above the level of the liquid culture of wt or mutant bacteria, for 18 hours. CBS/CSE and 3MST inhibitors PAG/AOAA (inh) and aspartate (Asp, 3.2 mM), respectively, were added as indicated. Numbers (%) show the relative decrease in H_2S production due to chemical or genetic inhibition of CBS/CSE and 3MST. p*MST* indicates the *E. coli* strain that expresses an extra copy of the 3MST gene under a strong pLtetO-1 promoter. (**B**) Cysteine (Cys) is a substrate for bacterial CBS/CSE and 3MST. Addition of Cys (25 μM for *E. coli*; 200 μM for other species) greatly stimulated H_2S synthesis in wt, but not in CBS/CSE- or 3MST-deficient strains. (**C**) H_2S suppresses antibiotic-mediated bacterial killing. Representative survival curves show the effect of CBS/CSE (*B. anthracis*) and 3MST (*E. coli*) deletions or CBS/CSE inhibition (*S. aureus* and *P. aeruginosa*) by PAG/AOAA (inh) on Gm-mediated (50 μg/ml) killing. Where indicated, NaHS (0.2 mM) was added before the antibiotic challenge (see Materials and Methods). The percentage of surviving cells was determined by counting colony-forming units (CFU) and is shown as the mean ± SD from three experiments.

Formation of double-strand DNA breaks (DSBs) is the primary cause of bacterial death from peroxide (*12*, *13*). These DSBs result from the Fenton reaction (*14*), which can also be triggered by antibiotics (*8*, *10*, *15*, *16*). To examine whether H_2S protects bacteria from the damaging Fenton reaction, we monitored chromosomal DNA integrity by pulsed-field gel electrophoresis (PFGE) (Fig. 2D). The intact *E. coli* chromosome does not migrate into the agarose gel but remains at the origin (*17*), whereas linear chromosomes containing a single DSB migrate as a 4.6-Mb species (Fig. 2D, lane 1). Absent antibiotic or H_2O_2, DNA isolated from wt or H_2S-deficient cells was retained almost entirely at the origin (lanes 2 and 3). However, treatment of cells with a sublethal dose of H_2O_2 or ampicillin resulted in a greater linearization (DSBs) of the chromosome in 3MST-deficient cells (lanes 4 and 6). Overexpression of 3MST suppressed this linearization (lane 8), as did treatment with NaHS (lanes 9 and 10). These results were corroborated by polymerase chain reaction (PCR) analysis of *B. anthracis*, *E. coli*, *and P. aeruginosa* genomic DSBs as a function of H_2S production (fig. S12) and further supported by the ability of H_2S to suppress the Gm-induced SOS response (fig. S13). Taken together, these results directly implicate endogenous H_2S in the mitigation of chromosomal damage inflicted by antibiotics.

The antioxidant effect of endogenous H_2S can also be explained, in part, by its ability to augment the activities of catalase and superoxide dismutase (SOD) (Fig. 2E). The rate of H_2O_2 degradation in crude extracts of wt *E. coli* cells was >1.5 times that of 3MST-deficient cells and was increased further in cells that overexpressed 3MST (Fig. 2E). SOD activity was also proportional to the level of 3MST expression (Fig. 2E).

Thus, H_2S increases bacteria resistance to oxidative stress and antibiotics by a dual mechanism (fig. S14) of suppressing the DNA-damaging Fenton reaction via Fe^{2+} sequestration (Fig. 2A and figs. S10 and S15) and stimulating the major antioxidant enzymes catalase and SOD (Fig. 2E). The latter is essential for long-term protection but is less important during the first moments of oxidative stress. Indeed, *kat*E and *sod*A *E. coli* mutants are well protected by NaHS during the first minutes of H_2O_2 exposure but then quickly loose viability (Fig. 2F).

This cytoprotective mechanism of H_2S parallels that of NO (*8*), which suggests that bacteria that produce both gases may benefit from their synergistic action. To test this hypothesis, we examined the effect of simultaneously inhibiting H_2S and NO on *B. anthracis* growth. We were unable to generate a strain of *B. anthracis* in which both bacterial nitric oxide synthase (bNOS) and CBS/CSE were genetically inactivated, which suggested that the absence of both gases is incompatible with *B. anthracis* survival. Indeed, *B. anthracis* Δ*nos* cells containing an isopropyl-β-D-thiogalactopyranoside (IPTG)–inducible CBS/CSE conditional knockout could grow only in the presence of IPTG (fig. S16). Notably, the amount of NO produced in H_2S-deficient cells or the amount of H_2S produced in NO-deficient cells was greater than that produced in wt cells (Fig. 3A), which indicated that one gas compensates for the lack of the other. Also, the activity of both CBS/CSE and bNOS was stimulated in response to antibiotics (Fig. 3A). Moreover, H_2O_2 and antibiotics (e.g., erythromycin) substantially induced CBS/CSE gene expression (Fig. 3B) and H_2S production (Fig. 3B and fig. S17). Furthermore, chemical inhibition of CBS/CSE in bNOS-deficient cells or inhibition of bNOS in CBS/CSE-deficient cells sensitized *B. anthracis* to antibiotics to a much greater extent than did each mutation alone (Fig. 3C). These results in concert with our previous study (*8*) demonstrate the synergistic and specific protective effects of H_2S and NO against antibiotics. Notably, in contrast to bNOS, which is present in only a small number of Gram-positive species (*18*), H_2S enzymes are essentially universal (fig. S1). Because H_2S equilibrates rapidly across cell membranes, a fraction of cells that generate this gas in culture or in biofilms could, in principle, defend the entire population. Indeed, wt *E. coli* cells effectively protect 3MST-deficient cells from Gm toxicity in exponentially growing coculture (fig. S18).

Because endogenous H_2S diminishes the effectiveness of many clinically used antibiotics, the inhibition of this "gaskeeper" should be considered as an augmentation therapy against a broad range of pathogens. Bacterial CBS, CSE, and 3MST have diverged substantially from their mammalian counterparts (fig. S2), which suggest that it is possible to design specific inhibitors targeting these enzymes.

Table 1. 3MST protects *E. coli* against different classes of antibiotics. A representative list of chemicals from the Phenotype MicroArray that preferentially suppressed the growth of 3MST-deficient cells (Δ*sseA*). Major classes of antibiotics are indicated by type (column 4). Negative numbers indicate the relative growth inhibition of the 3MST-deficient strain compared with that of the wt strain (as provided by Biolog Inc.) (fig. S4). The minimum inhibitory concentration drop for Δ*sseA*, as determined by Biolog, for two representative antibiotics, norfloxacin and troleandomycin, is 12- and 7-fold, respectively.

Δ*sseA* inhibition	Chemical	Biological effect	Type
−265	Novobiocin	DNA intercalation	Quinolone
−212	Norfloxacin	DNA intercalation	Quinolone
−183	Nalidixic acid	DNA intercalation	Quinolone
−117	Oxolinic acid	DNA intercalation	Quinolone
−295	Acriflavine	DNA intercalation	Acridine
−142	9-Aminoacridine	DNA intercalation	Acridine
−93	Proflavine	DNA intercalation	Acridine
−372	Trifluoperazine	DNA intercalation	Phenothiazine
−262	Promethazine	DNA intercalation	Phenothiazine
−251	Chlorpromazine	DNA intercalation	Phenothiazine
−421	Streptomycin	Protein synthesis	Aminoglycoside
−179	Apramycin	Protein synthesis	Aminoglycoside
−520	Tylosin	Protein synthesis	Macrolide
−498	Oleandomycin	Protein synthesis	Macrolide
−468	Erythromycin	Protein synthesis	Macrolide
−294	Josamycin	Protein synthesis	Macrolide
−235	Spiramycin	Protein synthesis	Macrolide
−203	Troleandomycin	Protein synthesis	Macrolide
−136	Chloramphenicol	Protein synthesis	Amphenicol
−271	Fusidic acid	Protein synthesis	Steroid
−352	Rifamycin SV	RNA synthesis	Ansamycin
−212	Trimethoprim	DNA-RNA synthesis	Antifolate
−429	2,4-Diamino-6,7-diisopropylpteridine	DNA-RNA synthesis	Antifolate
−231	Polymyxin B	Membrane	Polymyxin
−102	Colistin	Membrane	Polymyxin
−198	Vancomycin	Cell wall	Glycopeptide
−201	Cefsulodin	Cell wall	Cephalosporin
−160	Cephalothin	Cell wall	Cephalosporin
−159	Cefoperazone	Cell wall	Cephalosporin
−346	Oxacillin	Cell wall	Lactam
−227	Nafcillin	Cell wall	Lactam
−216	Phenethicillin	Cell wall	Lactam
−186	Penicillin G	Cell wall	Lactam
−182	Cloxacillin	Cell wall	Lactam
−171	Moxalactam	Cell wall	Lactam
−164	Carbenicillin	Cell wall	Lactam

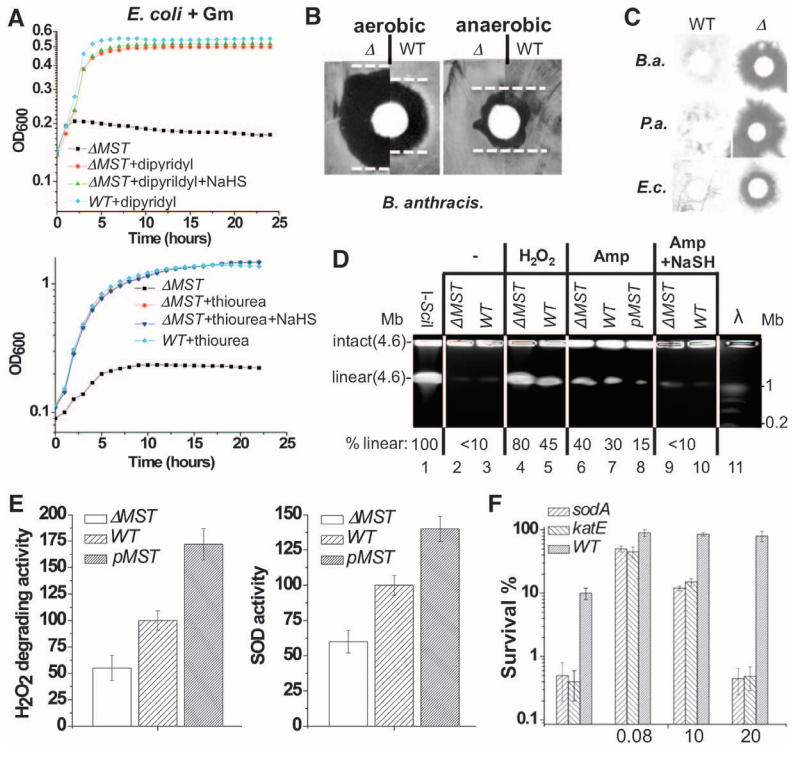

Fig. 2. H_2S protects against antibiotic-inflicted oxidative damage (**A**) H_2S acts by diminishing reactive oxygen species (ROS)–mediated antibiotic toxicity. *E. coli* cells were pretreated with the iron chelator, 2,2′-dipyridyl (0.05 mM) or the ROS scavenger thiourea (15 mM) for 3 min, followed by treatment with Gm. Cells were grown in triplicate at 37°C with aeration using a Bioscreen C automated growth analysis system. The curves represent averaged values from three parallel experiments with a margin of error of less than 5%. (**B**) Endogenous H_2S renders cells more resistant to NA in aerobic conditions, but fails to do so in anaerobic conditions. A paper disk saturated with 20 μg/ml NA was placed on wt or CBS/CSE-deficient *B. anthracis* lawns that were grown aerobically or anaerobically for the next 18 hours. Zone borders are marked with dashed lines. (**C**) Endogenous H_2S renders bacteria resistant to hydrogen peroxide. Agar plates seeded with the indicated bacteria were incubated overnight with a filter paper disk saturated with 0.125 or 0.45 M H_2O_2 placed atop the bacterial lawn. CBS/CSE- or 3MST-deficient cells formed a clear 5- to 10-mm zone around the disk, whereas wt cells grew a complete lawn and so demonstrated strong H_2S-dependent resistance to hydrogen peroxide. (**D**) Pulsed-field gel analysis of chromosomal DSBs. Lane 1: 4.6 Mb linearized *E. coli* chromosomes (*I-SceI*); lanes 2 and 3: DNA from wt and Δ*MST* cells; lanes 6 to 8: DNA from wt, 3MST-deficient, and 3MST-overproducing cells after treatment with 10 μg/ml Amp; lanes 9 and 10: DNA from NaHS-treated cells after Amp treatment; and lane 11: concatemers from 0.05 to 1.0 Mb. "% linear" indicates the relative increase in linearized chromosomal DNA. The values are the average of three independent experiments ($P < 0.1$). (**E**) Stimulating effect of H_2S on H_2O_2 degrading activity and SOD activity in crude extracts of wt and 3MST-deficient *E. coli* cells. Total H_2O_2 degrading activity was measured as described in (*7*). Catalase activity at 100% is 30 mM H_2O_2 min^{-1}•mg^{-1}. Values shown are the means ± SEM from three experiments. SOD activity was measured using a tetrazolium-based assay kit. (**F**) Dual protective effect of H_2S against oxidative stress: Catalase and SOD are required for prolonged defense against H_2O_2 toxicity mediated by NaHS but not for immediate protection. Wt, *kat*E, and *sod*A *E. coli* cells were grown in Luria-Bertani broth (LB) to absorbance (optical density) OD_{600} of ~1.0, treated with NaHS (200 μM) for the indicated time intervals (min), followed by the addition of H_2O_2 (2 mM) for 10 min. Cell survival was determined by counting CFU and is shown as the mean ±SD from three independent experiments.

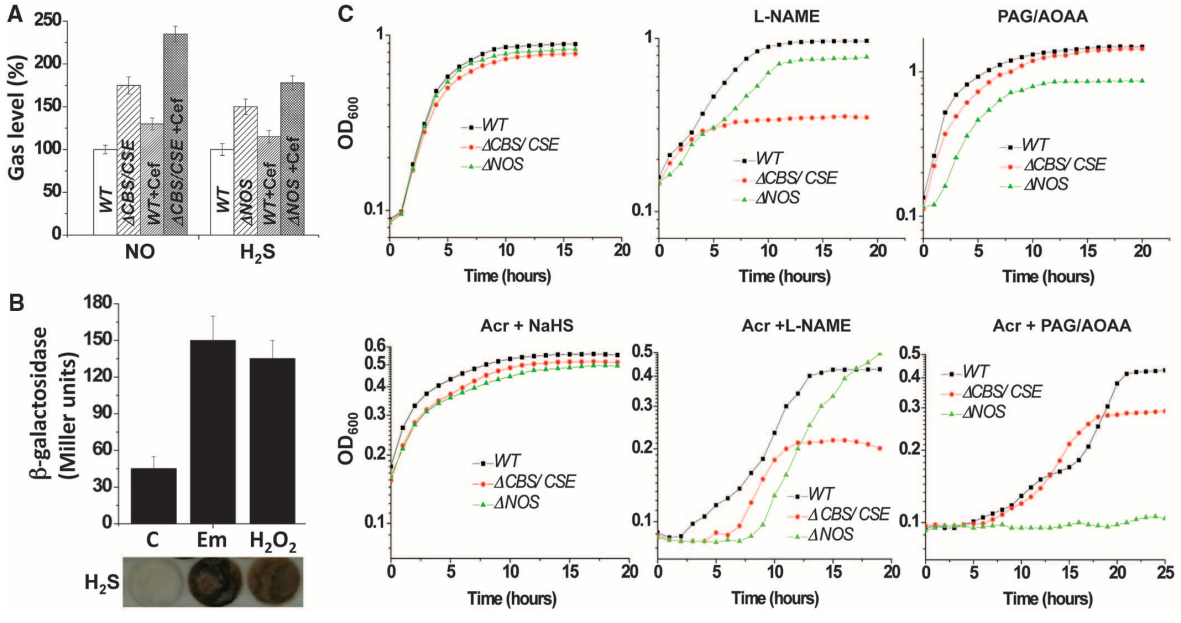

Fig. 3. Synergistic action of H_2S and NO in *B. anthracis*. (**A**) Compensatory induction of endogenous H_2S and NO. In vivo production of NO in response to deletion of CBS/CSE or cefuroxime (Cef) (20 μg/ml) challenge was detected using the Cu(II)-based NO fluorescent sensor (CuFL) (*19*) (left bars). Cells were grown in LB to OD_{600} of ~0.5 followed by addition of freshly prepared CuFL (20 μM) and Cef. Fluorescence was measured in the total culture after 18 hours of incubation using a real-time fluorometer (PerkinElmer LS-55). H_2S was measured using $Pb(Ac)_2$ as in Fig. 1A (right bars). (**B**) H_2S induction in response to antibiotic (erythromycin) or H_2O_2 challenge. The plot shows β-galactosidase activity (Miller units) expressed by *B. anthracis* cells harboring a chromosomal transcriptional fusion of the *cbs/cse* promoter and leader region to a promoterless *lacZ* gene. Bacteria were grown in LB medium until OD_{600} of ~0.6 followed by the addition of 0.5 μg/ml erythromycin or 2 mM H_2O_2. The bottom panel shows PbS brown or black stain, which is proportional to the amount of H_2S produced. *B. anthracis* cells were grown in 96-well plates in LB + Cys (200 μM) covered with lead acetate–soaked paper by using a Bioscreen C automated growth analysis system. (**C**) Representative OD growth curves of wt (black curves), CBS/CSE-deficient (red) or bNOS-deficient (green) *B. anthracis* (Sterne) cells. Acriflavine, PAG/AOAA, NaSH, and the NOS inhibitor *N*-nitro-L-arginine methyl ester (L-NAME) were added as indicated. Cells were grown in triplicate at 37°C with aeration using a Bioscreen C automated growth analysis system. The curves represent the averaged values ($P < 0.05$).

References and Notes

1. H. Kimura, *Antioxid. Redox Signal.* **12**, 1111 (2010).
2. M. M. Gadalla, S. H. Snyder, *J. Neurochem.* **113**, 14 (2010).
3. R. Wang, *Antioxid. Redox Signal.* **12**, 1061 (2010).
4. A. K. Mustafa, M. M. Gadalla, S. H. Snyder, *Sci. Signal.* **2**, re2 (2009).
5. B. Lima, M. T. Forrester, D. T. Hess, J. S. Stamler, *Circ. Res.* **106**, 633 (2010).
6. I. Gusarov, E. Nudler, *Proc. Natl. Acad. Sci. U.S.A.* **102**, 13855 (2005).
7. K. Shatalin *et al.*, *Proc. Natl. Acad. Sci. U.S.A.* **105**, 1009 (2008).
8. I. Gusarov, K. Shatalin, M. Starodubtseva, E. Nudler, *Science* **325**, 1380 (2009).
9. B. A. Forbes, *Bailey and Scott's Diagnostic Microbiology* (Mosby, St. Louis, MO, ed. 10, 1998).
10. M. A. Kohanski, D. J. Dwyer, B. Hayete, C. A. Lawrence, J. J. Collins, *Cell* **130**, 797 (2007).
11. N. R. Asad, A. C. Leitão, *J. Bacteriol.* **173**, 2562 (1991).
12. O. I. Aruoma, B. Halliwell, E. Gajewski, M. Dizdaroglu, *J. Biol. Chem.* **264**, 20509 (1989).
13. S. I. Liochev, I. Fridovich, *IUBMB Life* **48**, 157 (1999).
14. J. A. Imlay, *Annu. Rev. Microbiol.* **57**, 395 (2003).
15. M. A. Kohanski, D. J. Dwyer, J. J. Collins, *Nat. Rev. Microbiol.* **8**, 423 (2010).
16. B. W. Davies *et al.*, *Mol. Cell* **36**, 845 (2009).
17. B. Birren, E. Lai, *Pulsed-Field Gel Electrophoresis: A Practical Guide* (Academic Press, New York, 1993).
18. I. Gusarov *et al.*, *J. Biol. Chem.* **283**, 13140 (2008).
19. M. H. Lim, D. Xu, S. J. Lippard, *Nat. Chem. Biol.* **2**, 375 (2006).

Acknowledgments: We thank E. Avetissova for technical assistance, S. Mashko for materials, and members of the Nudler laboratory for valuable comments and discussion. This research was supported by the NIH Director's Pioneer Award, Biogerontology Research Foundation, and Dynasty Foundation (E.N.). Provisional patent application has been filed: U.S. Patent No. 61/438,524 "Methods for treating infections by targeting bacterial H_2S-producing enzymes." by K.S. and E.N.

Supporting Online Material

www.sciencemag.org/cgi/content/full/334/6058/986/DC1
Materials and Methods
SOM Text
Figs. S1 to S20
Table S1
References (*20*–*34*)

15 June 2011; accepted 14 September 2011
10.1126/science.1209855

Wolbachia Enhance *Drosophila* Stem Cell Proliferation and Target the Germline Stem Cell Niche

Eva M. Fast,[1] Michelle E. Toomey,[1,2] Kanchana Panaram,[1] Danielle Desjardins,[1]* Eric D. Kolaczyk,[3] Horacio M. Frydman[1,2]†

Wolbachia are widespread maternally transmitted intracellular bacteria that infect most insect species and are able to alter the reproduction of innumerous hosts. The cellular bases of these alterations remain largely unknown. Here, we report that *Drosophila mauritiana* infected with a native *Wolbachia w*Mau strain produces about four times more eggs than the noninfected counterpart. *Wolbachia* infection leads to an increase in the mitotic activity of germline stem cells (GSCs), as well as a decrease in programmed cell death in the germarium. Our results suggest that up-regulation of GSC division is mediated by a tropism of *Wolbachia* for the GSC niche, the cellular microenvironment that supports GSCs.

Wolbachia are maternally transmitted intracellular bacteria infecting a large number of invertebrates such as insects and parasitic worms (*1*). Many invertebrates that harbor these bacteria are either the vectors (for instance, mosquitoes) or the causative agent (for example, filarial nematodes) of devastating human infectious diseases. By understanding the biology at the interface between *Wolbachia* and their hosts, advances in the treatment of filarial diseases and the control of disease vectors are made possible (*2*–*7*). Furthermore, *Wolbachia* can dramatically alter host reproduction, affecting the evolutionary history of numerous invertebrates (*1*). Therefore, understanding how *Wolbachia* affect their hosts is an important ecological, evolutionary, and human health question.

To investigate the influence of *Wolbachia* on their hosts at the cellular level, we used the *Drosophila* gonad, a powerful experimental system. We have previously shown that in *Drosophila melanogaster*, *Wolbachia* target the somatic stem cell niche (SSCN) (Fig. 1A), the microenvironment that supports the somatic stem cells, in the female ovary (*8*). Further work shows that *Wolbachia* also target the somatic stem cell niche in the ovary of other insects (*9*, *10*). Here, we report two additional stem cell niches preferentially colonized (i.e., cell tropism) by *Wolbachia*: the female germline stem cell niche (GSCN) (Fig. 1A) and the hub, at the apical tip of the testis (discussed below). In a *D. mauritiana* stock infected with *Wolbachia w*Mau, we consistently noticed an intense accumulation of bacteria in the GSCN, the structure harboring the GSCs (infection frequency = 91 ± 5.7%, N = 958 germaria) (see *Wolbachia*, labeled green in Fig. 2, A and B, Fig. 3A, and fig. S1A). This GSCN accumulation was absent in *D. melanogaster* (GSCN infection frequency = 0%, N = 180 germaria) (see fig. S1, B compared to A). Electron microscopy (EM) and three-dimensional reconstruction of confocal images show that the vast majority of the cytoplasmic volume of the GSCN is occupied by *Wolbachia w*Mau [see Fig. 1B, the *Wolbachia* cells (a red asterisk indicates a single bacterial cell) occupy most of the GSCN (shown in green) compared with the noninfected control in fig. S1C; see also movie S1]. Because GSCN function is essential for stem cell maintenance and activity (*11*), we hypothesized that the high levels of infection in the niche would impair its associated stem cells to a certain degree. An easy readout of GSC activity is egg production, because every egg produced originates from the division of a stem cell associated with the GSCN (Fig. 1A′). The total number of eggs laid per *Wolbachia*-infected female was 3.5 times higher than that observed in noninfected flies (herein referred to as "W–"; the genetic background of the W– flies was homogenized by successive backcrossing to infected males, as shown in fig. S2). This experiment was repeated under different temperature, humidity, and age conditions [see supporting online material (SOM) methods and table S1] (*12*). Under these different conditions, infected flies (W+) still produced approximately fourfold more eggs than the noninfected females (Fig. 1C and table S1).

Given these levels of egg production, we reasoned that W+ ovaries contain GSCs that are more active. To test this possibility, we measured the frequency of GSC division in W+ and W– flies using three different markers for three distinct phases of the cell cycle. We performed the initial assessment with the use of an antibody to phospho-histone H3, which labels cells in mitosis (Fig. 2, A and C, and fig. S3G) (*12*). The labeling of GSCs in W+ flies was, on average, 2.7 (± 0.23)–fold higher than in W– flies (Fig. 2E and table S2). This increase could indicate either a higher GSC division in infected germaria or an arrest during the mitotic phase of the cell cycle.

We further investigated GSC proliferation using two additional markers: incorporation of the thymidine analog BrdU, an indicator of DNA synthesis during S phase (fig. S3, A, D, and G), and a particular fusome morphology characteristic of GSCs in G_2 (fig. S3, B, E, and H). The fusome is a germline-specific organelle that assumes the shape of an exclamation mark (!) during G_2 (*13*, *14*). Both markers corroborated a higher GSC proliferation rate in W+ (Fig. 2E). In nine independent experiments using three different methods, stem cell division in W+ flies was, on average, doubled (2.12 ± 0.66) (table S2). For

[1]Department of Biology, Boston University, Boston, MA 02215, USA. [2]National Emerging Infectious Disease Laboratory, Boston University, Boston, MA 02118, USA. [3]Department of Mathematics and Statistics at Boston University, Boston, MA 02215, USA.

*Present address: Medical University of South Carolina, Charleston, SC 29412, USA.

†To whom correspondence should be addressed. E-mail: hfrydman@bu.edu